



# Clinical Utility and Performance of an Ultrarapid Multiplex RNA-Based Assay for Detection of *ALK*, *ROS1*, *RET*, and *NTRK1/2/3* Rearrangements and *MET* Exon 14 Skipping Alterations



Ying-Hsia Chu,<sup>\*</sup> Jada Barbee,<sup>\*</sup> Soo-Ryum Yang,<sup>\*</sup> Jason C. Chang,<sup>\*</sup> Priscilla Liang,<sup>\*</sup> Kerry Mullaney,<sup>\*</sup> Roger Chan,<sup>\*</sup> Paulo Salazar,<sup>\*</sup> Ryma Benayed,<sup>\*</sup> Michael Offin,<sup>†</sup> Alexander Drilon,<sup>†‡</sup> Marc Ladanyi,<sup>\*</sup> Khedoudja Nafa,<sup>\*</sup> and Maria E. Arcila<sup>\*</sup>

From the Department of Pathology and Laboratory Medicine,<sup>\*</sup> Molecular Diagnostic Service, and the Thoracic Oncology Service,<sup>†</sup> Division of Solid Tumor Oncology, Department of Medicine, Memorial Sloan Kettering Cancer Center, New York; and the Department of Medicine,<sup>‡</sup> Weill Cornell Medical College, New York, New York

Accepted for publication  
March 3, 2022.

Address correspondence to Maria E. Arcila, M.D., Department of Pathology and Laboratory Medicine, Molecular Diagnostic Service, Memorial Sloan Kettering Cancer Center, 1275 York Ave., New York, NY 10065.  
E-mail: [arcilam@mskcc.org](mailto:arcilam@mskcc.org).

Several kinase fusions are established targetable drivers in lung cancers. However, rapid and comprehensive detection remains challenging because of diverse partner genes and breakpoints. We assess the clinical utility and performance of a rapid microfluidic multiplex real-time PCR-based assay for simultaneous query of fusions involving *ALK*, *ROS1*, *RET*, and *NTRK1/2/3*, as well as *MET* exon 14 skipping, using a 3-hour automated process. Dual analytic strategies were utilized: fusion-specific amplification and 3' to 5' expression imbalance. One-hundred and forty-three independent, formalin-fixed, paraffin-embedded tumor samples (112 surgical specimens, 31 cytologic cell blocks) were analyzed: 133 with known kinase gene alterations and 10 negative samples based on clinically validated next-generation sequencing. Testing was successful in 142 (99%) cases. The assay demonstrated a sensitivity of 97% (28/29), 100% (31/31), 92% (22/24), 81% (22/27), and 100% (20/20) for *ALK*, *RET*, *ROS1*, and *NTRK1/2/3* rearrangements and *MET* exon 14 skipping alterations, respectively, with 100% specificity for all. Concordant results were achieved in specimens aged up to 5 years, with >10% tumor, and inputs of at least 9 mm<sup>2</sup> (surgical specimens) and 9000 cells (cytologic cell blocks). The assay enables rapid screening for clinically actionable kinase alterations with quicker turnaround and lower tissue requirements compared with immunohistochemistry and molecular methods, while also circumventing the infrastructure dependencies associated with next-generation sequencing and fluorescence *in situ* hybridization. (*J Mol Diagn* 2022, 24: 642–654; <https://doi.org/10.1016/j.jmoldx.2022.03.006>)

Gene rearrangements affecting several receptor tyrosine kinases (RTKs) are important targetable oncogenic alterations in lung cancer. Therapeutically actionable gene fusions drive approximately 10% of non-small-cell lung

cancers (NSCLCs).<sup>1,2</sup> In most cases, the 3' region (kinase domain) of the kinase gene fuses with a 5' partner gene that may provide dimerization domains. This enables ligand-independent dimerization and activation, leading to

Supported by the Comprehensive Cancer Center Core grant P30 CA008748 at Memorial Sloan Kettering Cancer Center from the NIH.

K.N. and M.E.A. contributed equally to this work.

Disclosures: R.B. has received a grant and travel credit from ArcherDx, honoraria for advisory board participation from Loxo Oncology and Roche Dx, speaking fees from Illumina, and consulting fees from Hitachi. A.D. has received honoraria or worked on the advisory boards of Ignyta/Genentech/Roche, Loxo/Bayer/Lilly, Takeda/Ariad/Millennium, TP Therapeutics,

AstraZeneca, Pfizer, Blueprint Medicines, Helsinn, Beigene, BergenBio, Hengrui Therapeutics, Exelixis, Tyra Biosciences, Verastem, MORE Health, Abbvie, 14ner/Elevation Oncology, Remedica Ltd., ArcherDX, Monopteros, Novartis, EMD Serono, Medendi, Liberum, Repare RX, Nuvalent, Merus, AXIS, Chugai Pharm, EPG Health, and Harborside Nexus; has received funding through his institution from Pfizer, Exelixis, GlaxoSmithKline, Teva, Taiho, and PharmaMar; has received research support from Foundation Medicine; receives royalties from Wolters Kluwer; has received other

downstream deregulation of cell proliferation and survival. In other oncogenic fusions, 3' kinase domain overexpression may result from promoter swapping or loss of autoinhibitory domain.<sup>3</sup> The most common RTK fusions in NSCLC involve *ALK* (3.5%), *ROS1* (2.7%), and *RET* (1.7%).<sup>4</sup> More recently, fusions involving the neurotrophic tropomyosin receptor family of RTKs (*NTRK1*, *NTRK2*, and *NTRK3*) have been reported in 0.2% of lung adenocarcinomas, while occurring at high frequency (>90%) in rare tumors, such as secretory carcinoma.<sup>5</sup> Another type of RTK alteration recently described is *MET* exon 14 skipping, an intragenic rearrangement of *MET* occurring in approximately 3% of NSCLCs.<sup>6</sup> In this case, mutations affecting the splicing acceptor and donor sites of exon 14 lead to skipping of the exon and generation of a shorter protein with characteristic in-frame deletion of the juxtamembrane domain. Of note, up to 40% of rearrangement-driven lung cancers are diagnosed at an advanced stage (III to IV),<sup>1,2,7</sup> complicated by severe respiratory distress due to diffuse lung parenchymal involvement and/or malignant airway obstruction in many cases.<sup>8–11</sup> Fortunately, tyrosine kinase inhibitor therapy typically induces rapid and profound clinical improvement.<sup>8–12</sup> Timely recognition of these alterations, particularly in symptomatic patients or in those with an extensive disease burden, is thus critical in the clinic.

Laboratory detection of rearrangements involving RTKs may be challenging because of their complex biology. For *MET* alterations, both RNA- and DNA-based sequencing approaches may be used; DNA approaches target the detection of mutations predicted to lead to exon 14 skipping, whereas RNA approaches detect the direct fusion of exon 13 and exon 15 transcripts. Detection of kinase fusions is more complex. Common methods include fluorescence *in situ* hybridization (FISH), quantitative real-time PCR, and next-generation sequencing (NGS), each with intrinsic limitations and variably long turnaround times (TATs). Alternatively, protein expression by immunohistochemistry (IHC) may be used as a surrogate for rapid detection with more favorable TATs. Commercial IHC antibodies are available for determining *ALK*, *ROS1*, *RET*, and *NTRK* (pan-TRK) expression. However, unlike *ALK* IHC, which predicts fusion with sensitivity and specificity of nearly 100%,<sup>13,14</sup> other kinase-based IHC analyses show heterogeneous, partner gene-dependent performance. For example, although Solomon et al<sup>5</sup> reported an overall sensitivity and specificity of 88% and 81%, respectively, for pan-TRK IHC in a set of 87

*NTRK* fusion-positive tumors, sensitivity was lower in *NTRK3* (79%) compared with *NTRK1* (96%) and *NTRK2* (100%) fusion-positive tumors. Notably, false pan-TRK positivity may occur in tumors exhibiting neural or smooth muscle differentiation.<sup>15</sup> Similar heterogeneous performance with *RET* IHC was observed by Yang et al,<sup>16</sup> reporting sensitivities of 50% to 100%, depending on the fusion partner, and overall specificity of 82%. Despite a high sensitivity nearing 100%, *ROS1* IHC also demonstrates variable specificity of as low as 70%, limiting its use as a reliable rapid screening method.<sup>17</sup> FISH, which has traditionally served as the gold standard for gene rearrangement analysis, presents limitations related to low multiplexing capability and lack of functional resolution, such as the intactness of kinase domain and translational reading frames. Moreover, falsely negative break-apart FISH may occur in fusions generated by short-segment inversions (eg, *NCOA4::RET*<sup>16</sup> and *BIRC6::ALK*<sup>18</sup>) with visually undiscernible probe separation.<sup>16</sup>

In recent years, NGS has become the mainstay for high-throughput therapeutic target search. Despite a reduced per-gene analytic cost, most NGS assays require a TAT of 2 to 3 weeks and may not be broadly available. In addition, there are underlying genomic and biologic complexities that can lead to false-negative gene fusion results. When using DNA-based NGS analysis, the most common type of NGS testing done for lung cancer, some fusions may go undetected because of incomplete targeting. Concurrent or sequential testing by RNA-based NGS could be used to enhance detection, but RNA sequencing has yet to be adopted more broadly in routine clinical practice. Targeted NGS-based analysis of circulating tumor DNA typically requires at least 2 weeks of TAT, particularly when molecular barcoding and advanced bioinformatics are employed to ensure assay accuracy. Prior studies have reported heterogeneous pretreatment sensitivity (54% to 79%<sup>19,20</sup>) of circulating tumor DNA in detecting *ALK* fusions, likely due to variable tumor shredding.

More recently, the use of 3' to 5' expression imbalance has attracted scientific attention as a promising fusion detection method. In kinase fusion-driven tumors, oncogenic fusion transcripts are highly expressed and contain the 3' kinase domain-coding sequence. As a result, these tumors exhibit 3' to 5' expression imbalance (EI) of the rearranged kinase gene. EI can be queried using various

support from Boehringer Ingelheim; has received food/beverage from Merck, Puma, and Merus; and has received continuing medical education honoraria from Medscape, OncLive, PeerVoice, Physicians Education Resources, Targeted Oncology, Research to Practice, Axis, Peerview Institute, Paradigm Medical Communications, WebMD, MJH Life Sciences, Med Learning, Imedex, Answers in CME, and Clinical Care Options. M.O. reports personal fees from PharmaMar, Novartis, Targeted Oncology, Bristol-Myers Squibb, Merck Sharp, ASTRO, and Jazz Pharmaceuticals, outside the submitted work. M.L. reports personal fees from AstraZeneca, Bristol-Myers Squibb,

Takeda, Lilly Oncology, Blueprint Medicines, and Bayer; and grants from Loxo Oncology and Helsinn Healthcare, outside the submitted work. M.E.A. has received honoraria or worked on advisory boards for Janssen Global Services, Bristol-Myers Squibb, Roche, and AstraZeneca; has received speaker fees from Biocartis and Invivoscribe; and has received continuing medical education honoraria from OncLive, PeerVoice, Physicians Education Resources, Peerview Institute, and Clinical Care Options. All the other authors declare no conflict of interest.

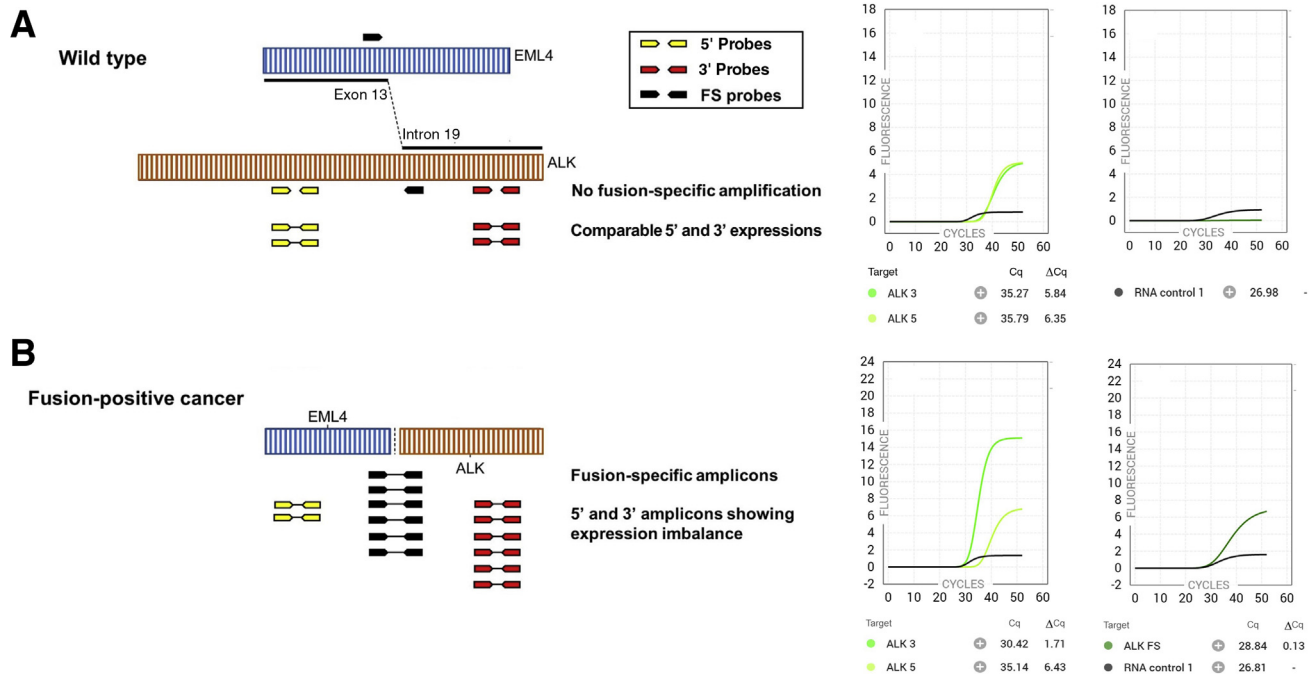


**Figure 1** The Idylla GeneFusion assay queries kinase gene rearrangements through quantitative real-time PCR using fusion-specific (FS) and expression imbalance (EI) primers and probes. **A:** In normal tissue and nonrearranged tumors, the 3' and 5' EI probes show similar levels of expression, whereas the FS probes fail to amplify. **B:** In fusion-driven tumors, overexpression of fusion transcripts causes 3' overexpression and, in cases harboring the targeted fusions listed in Supplemental Table S1, gives rise to fusion-specific amplicons. Corresponding representative plots for wild type and ALK fusion are seen on the right.

methods, such as direct RNA hybridization-based transcript enumeration (eg, NanoString nCounter<sup>21–26</sup>), quantitative RT-PCR (RT-qPCR),<sup>27,28</sup> digital PCR,<sup>29</sup> matrix-assisted laser desorption/ionization time-of-flight analysis,<sup>24</sup> and NGS,<sup>30,31</sup> with limited published experience in routine clinical practice. Some assay designs employ dual testing strategies to enhance detection, with multiple probe sets targeting not only the 5' and 3' regions of kinase gene for EI assessment, but also the most common gene breakpoints for the tumor type(s) of interest.<sup>21,22,24</sup>

Regardless of the method used, the complexity of testing and TAT requirements of molecular approaches have remained high, such that routine comprehensive, multigene assessment for fusions is only performed in a low proportion of cases and, even when performed, results may not be available in a therapeutically actionable time frame. Overall, there is an unmet need for a fusion detection method that is rapid, includes multigene coverage of the most frequent druggable kinase fusions, and can be easily established in routine practice across laboratories. This study set out to validate and determine the clinical utility of the Idylla GeneFusion test, a new microfluidic multiplexed RT-qPCR assay for concurrent query of ALK, ROS1, RET, NTRK1, NTRK2, and NTRK3 rearrangements and alterations that result in MET exon 14 skipping. Testing was performed in a large clinical sample series previously characterized by NGS. The assay's analytic sensitivity, limit of detection, and repeatability were also assessed using commercially available reference material, prequantified by NGS and digital PCR.

## Materials and Methods

### Sample Identification

Solid tumor cases with known kinase gene rearrangements involving ALK, ROS1, RET, or NTRK1/2/3, or with MET splice site alterations, were identified on the basis of results of routine clinical testing by Memorial Sloan Kettering–Integrated Mutation Profiling of Actionable Cancer Targets (MSK-IMPACT) (hybrid capture-based DNA NGS)<sup>32</sup> and MSK-Fusion (anchored multiplex PCR-based RNA NGS).<sup>33</sup> A broad range of samples was selected; positive samples harbored only one fusion or one MET exon 14 alteration, and each positive sample served as negative control for the other alterations. Ten negative cases were also included. All fusion events were manually reviewed using the Integrative Genomics Viewer<sup>34</sup> and JBrowse<sup>35</sup> to ensure in-frame coding, kinase domain intactness, and adequate read support, as previously described.<sup>32</sup> Electronic medical records were reviewed for tumor characteristics and treatment history. Formalin-fixed, paraffin-embedded (FFPE) tumor tissue blocks and corresponding whole-slide scanned images were retrieved from the Surgical Pathology and Cytopathology archives at the Memorial Sloan Kettering Cancer Center. Manual macrodissection for the Idylla assay was performed to enrich for tumor, when possible. This was guided to select the same regions previously macrodissected for nucleic extraction to perform MSK-IMPACT and MSK-fusion following the markings from the scanned whole-slide

images. Tumor purity was assessed by implementing the FACETS algorithm<sup>36</sup> on MSK-IMPACT sequencing output and correlated with the morphologic assessment by two board-certified pathologists (Y.H.C. and M.E.A.) based on hematoxylin and eosin slides. For surgical specimens, total tissue area of assay input was measured in whole-slide scanned images using a built-in tool of MSK Slide Viewer.<sup>37</sup> For cytology samples, cellularity was quantified using the QuPath cell detection tool<sup>38</sup> on whole-slide scanned images of hematoxylin and eosin-stained cell block sections (5 μm thick). Per-slide cellularity was multiplied by the number of slides used and rounded to the nearest thousand to estimate the total cellular input.

## Comparison Methods

Next-generation sequencing (NGS) assays served as the reference method, including MSK-IMPACT for all cases ( $N = 143$ ) and MSK-Fusion, performed in a subset of cases ( $N = 42$ ), as previously described.<sup>32,33</sup> MSK-IMPACT is a 505-gene DNA-based, hybrid-capture NGS panel with coverage of all exons and selected introns (In) of *ALK* (In 17 to 19; NM\_004304), *RET* (In7 to 11; NM\_020975), *ROS1* (In 30 to 35; NM\_002944), *NTRK1* (In 3 and 7 to 12; NM\_002529), *NTRK2* (In 15; NM\_006180), and *NTRK3* (NM\_001012338) (<https://www.ncbi.nlm.nih.gov/gene>, last accessed April 7, 2022). MSK-Fusion is a targeted RNA-based NGS panel utilizing anchored multiplex PCR technology and targeting selected regions of 123 genes, including *ALK* (exons 19 to 22), *RET* (exons 8 to 13), *ROS1* (exons 31 to 37), *NTRK1* (exons 8 to 13), *NTRK2* (exons 11 to 17), and *NTRK3* (exons 13 to 16). Both assays were fully validated for routine clinical diagnostic purposes.<sup>32,33</sup>

*ALK* IHC was performed in all cases as part of routine workup, whereas break-apart FISH was performed on selected cases to resolve discordant results. For IHC, immunohistochemical antibodies (clone D5F3, prediluted; Cell Signaling, Danvers, MA) were applied on FFPE sections (5 μm thick) and processed by an automated stainer (Leica, Buffalo Grove, IL). Break-apart FISH was performed using commercial probes for *ALK* (Abbott Molecular, Des Plaines, IL) on FFPE sections (5 μm thick). At least 100 valid nuclei were evaluated in each case. Cutoff for maximal allowable normal variation was 10%.

## Idylla GeneFusion Assay

The Idylla GeneFusion assay (Biocartis, Mechelen, Belgium) is a multiplex RT-qPCR assay designed for concurrent analysis of *ALK*, *ROS1*, *RET*, and *NTRK1/2/3* rearrangements and *MET* exon 14 skipping in 3 hours without pre-extraction. Automation is achieved through integrated microfluidic, cartridge-based, closed devices where whole nucleic acid extraction, reverse transcription, amplification, and detection take place. Each cartridge (single-sample/

**Table 1** Clinicopathologic Characteristics of the Samples ( $N = 143$ )

Characteristic	<i>n</i>	%
Age at diagnosis, median (range), years	63 (3–87)	
Sex, female/male (ratio)	97/46 (2:1)	
Primary tumor site		
Lung	108	76
Thyroid	17	12
Colon	6	4
Salivary gland	5	3
Soft tissue	4	3
Pancreas	2	1
Brain	1	<1
Distant metastasis (M1) at diagnosis	58	41
Kinase inhibitor therapy	55	38
Kinase gene alterations		
<i>ALK</i> fusions	29	22
<i>NTRK1</i> fusions	12	9
<i>NTRK2</i> fusion	1	1
<i>NTRK3</i> fusions	16	12
<i>RET</i> fusions	31	23
<i>ROS1</i> fusions	24	18
<i>MET</i> exon 14 skipping	20	15
No fusions or <i>MET</i> exon 14 skipping	10	7
Reference methods		
MSK-IMPACT alone	101	71
MSK-IMPACT and MSK-Fusion	42	29
Reference method turnaround time, median (range), days		
MSK-IMPACT	20 (10–89)	
MSK-Fusion	8 (4–18)	

MSK-IMPACT, Memorial Sloan Kettering—Integrated Mutation Profiling of Actionable Cancer Targets.

single-use device) is manually loaded with unextracted FFPE tissue sections into a lysis chamber and loaded onto an Idylla instrument, with a technical hands-on time of approximately 2 minutes. In this study, samples were first tested using one tissue section (5 μm thick) per surgical case or five cell block sections per cytology specimen. In cases with borderline or invalid results (detailed below), testing was re-attempted with more sections, when available. Macrodissection was performed, whenever feasible, for maximal tumor enrichment. Driven by a fully automated workflow, liquefaction buffers are infused into the lysis chamber, where heat and high-intensity focused ultrasound are applied to further facilitate deparaffinization, cell lysis, and RNA de-cross-linking. Whole nucleic acids are purified using a chaotropic binding chemistry to a silica membrane and then eluted and transferred to five PCR chambers where multiplex RT-qPCR takes place using TaqMan PCR chemistry and fluorescence-based detection.

The analysis of gene fusions utilizes two technical modalities: detection of fusion-specific amplification and 3' to 5' expression imbalance (Figure 1). Fusion-specific (FS) primers were designed to amplify the flanking sequences of 93%, 97%, and 85% of *ALK*, *ROS1*, and *RET* fusion breakpoints, respectively, observed in lung

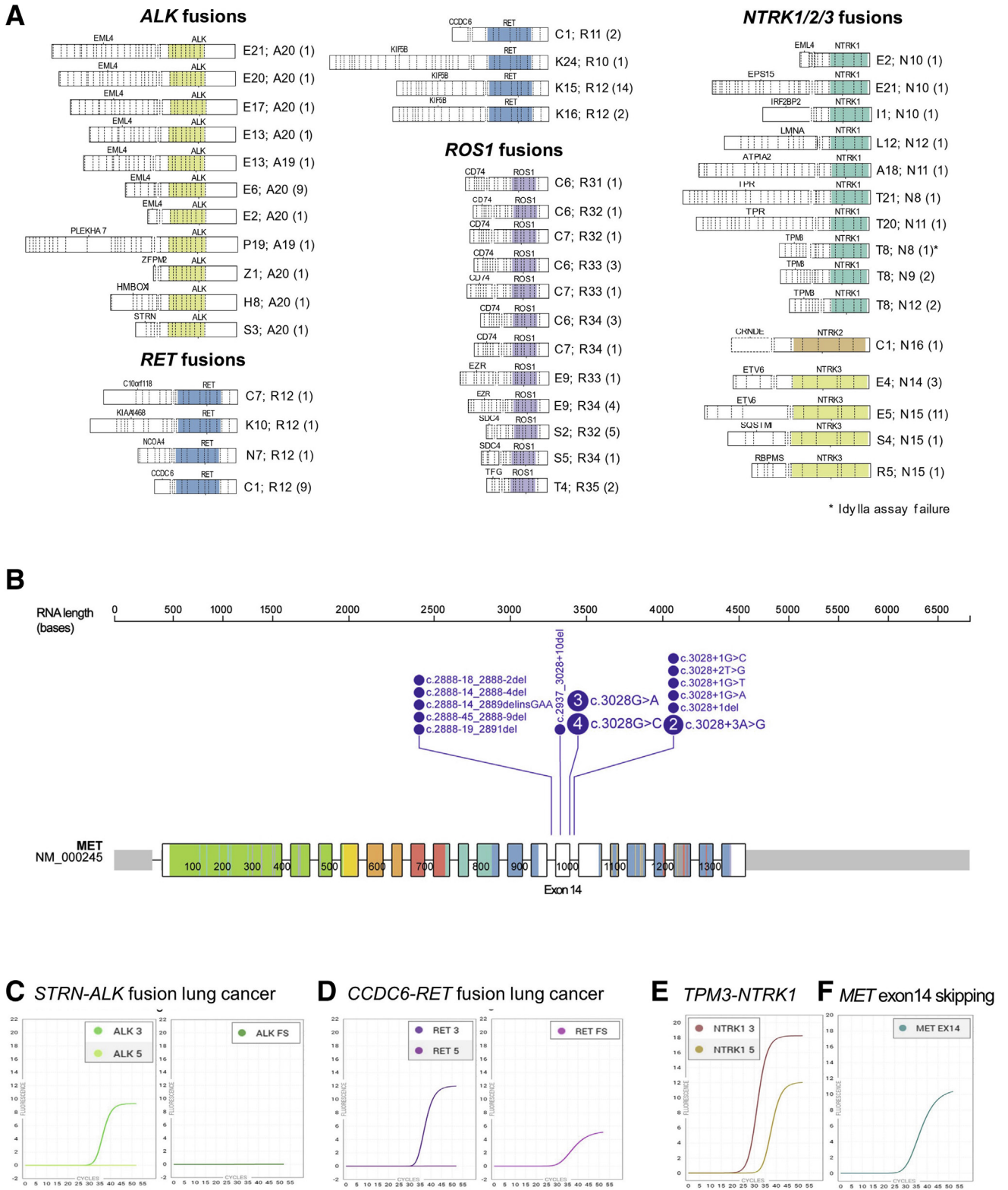


**Figure 2** Fusions and *MET* exon 14 skipping mutations included in the study. **A:** Fusions with the exon numbers involved in the breakpoints are listed alongside the transcripts with case numbers specified in parentheses. Transcript identifiers are listed in [Supplemental Tables S1 and S2](#). **B:** *MET* exon 14 skipping alterations tested (case numbers, if >1, are indicated in the circles). **C:** Representative plots of lung adenocarcinomas carrying a nontargeted *STRN-ALK* fusion shows expression imbalance with 3' curve alone and a  $\Delta Cq_{3'-HKG}$  of 2.11 (left); there was no fusion-specific (FS) amplification (right). **D:** A *CCDC6::RET* tumor shows positive FS detection in addition to expression imbalance with 3' curve alone ( $\Delta Cq_{3'-HKG} = 0.9$ ). **E:** Idylla detection of *NTRK* fusions relies solely on expression imbalance, which was seen in this *TPM3::NTRK1* fusion tumor with 3' overexpression. **F:** Dedicated probe sets for *MET* exon 14 skipping transcripts produce a clear fluorescent curve in this lung adenocarcinoma carrying *MET* c.3028 G>A mutation.

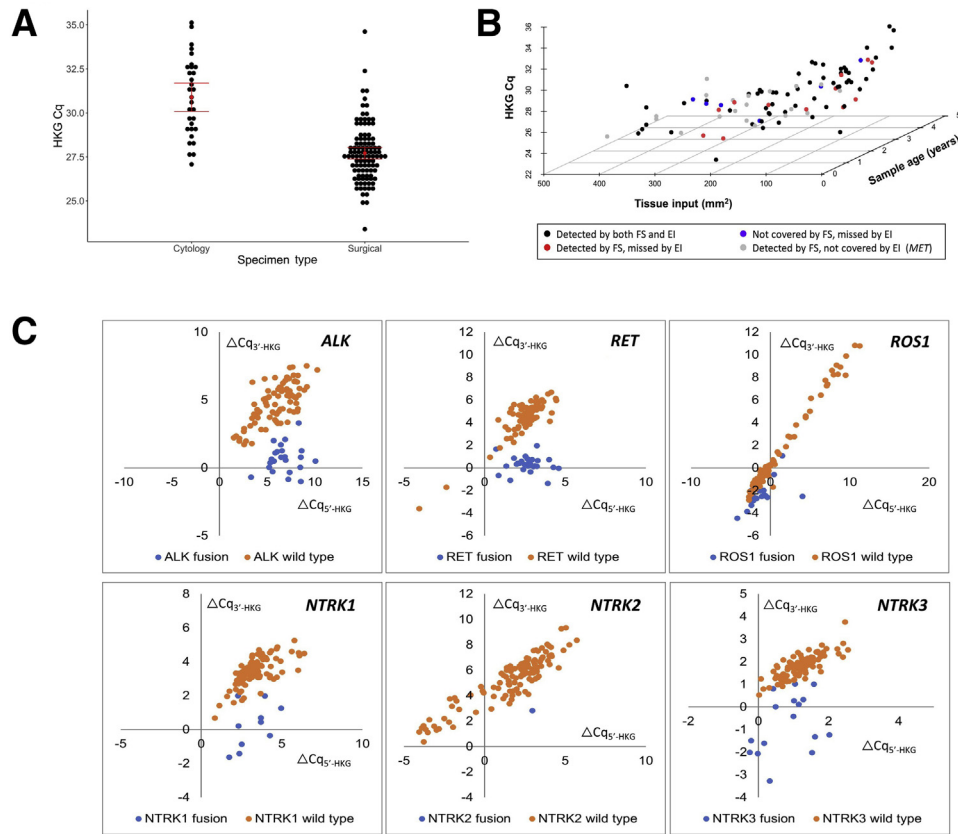


**Figure 3** Quality metrics and expression assessment. **A:** Distribution of  $Cq_{HKG}$  in the study. With higher cellular inputs, surgical specimens demonstrated overall lower  $Cq_{HKG}$  values compared with cytology specimens ( $P < 0.001$ ). The error bars indicate group-specific 95% CI based on a t-distribution. **B:** Distribution of  $Cq_{HKG}$  of surgical samples and the impact of sample age and overall input. As expected, older samples are associated with lower performance, but most still provide suitable quality metrics for fusion detection. **C:** Distribution of  $\Delta Cq_{5'-HKG}$  (x axis) and  $\Delta Cq_{3'-HKG}$  (y axis) in cases showing valid 3' and 5' curves. Distinct clustering of fusion-positive and wild-type samples was observed for *ALK* and *RET*. Note the comparable 3' and 5' expression levels in most wild-type samples, which roughly approximated a 45-degree ( $x \approx y$ ) line. For *ROS1*, most wild-type samples showed a high baseline expression with low  $\Delta Cq_{5'-HKG}$  and  $\Delta Cq_{3'-HKG}$ , which obscured the detection of expression imbalance in fusion-positive samples. Samples harboring *NTRK1*, *NTRK2*, and *NTRK3* showed variable degrees of 3' overexpression with reduced  $\Delta Cq_{3'-HKG}$  values compared with wild-type samples. Most of the samples with expression levels near the wild-type cluster had high tumor content. EI, expression imbalance; FS, fusion specific.

adenocarcinomas based on the Catalogue of Somatic Mutations in Cancer database<sup>39</sup> while also occurring in other cancer types (Supplemental Table S1<sup>40</sup>). In addition, both wild-type and exon 14 skipping variant transcripts of *MET* were interrogated with dedicated primer and probe sets, targeting adjoined regions of exons 13 and 15. EI analysis was performed to detect *NTRK1/2/3* fusions, as well as other rearrangements in *ALK*, *ROS1*, and *RET* that were not specifically targeted by FS primers and probes. Multiple probe sets to determine the 5' and 3' expression levels were employed, and the levels of expression were compared with the wild type expression of other samples in the cohort to establish optimal cutoffs. By design, the assay only identifies the presence of kinase gene rearrangements but does not determine the identity of the fusion partner even when amplified by the FS probes.

The RT-qPCR results were interpreted using the algorithm described in Supplemental Figure S1. Briefly, only amplification curves with a valid sigmoidal shape after fluorescent signal normalization were analyzed. Analysis began with

calculating a quantification cycle (Cq) value for each valid amplification curve. Overall assay validity was then determined on the basis of the Cq values of six PCRs targeting two housekeeping genes (HKGs), *TMUB2* and *ERCC3*, which were averaged into an overall housekeeping gene Cq ( $Cq_{HKG}$ ). For samples with acceptable  $Cq_{HKG}$ , each kinase gene was then interpreted independently. A positive fusion call was rendered when at least one of the following criteria was met:

- i) Valid FS amplification curve with acceptable Cq ( $Cq_{FS}$ ), or
- ii) Both 3' and 5' curves were valid with evident 3' overexpression based on the result of  $Cq_{3'}$  minus  $Cq_{5'}$  ( $\Delta Cq_{3'-5'}$ ), or
- iii) Only the 3' curve was valid in the absence of 5' curve, with evident 3' overexpression based on the result of  $Cq_{3'}$  minus  $Cq_{HKG}$  ( $\Delta Cq_{3'-HKG}$ ).

The interpretation cutoff values for  $Cq_{HKG}$ ,  $Cq_{FS}$ ,  $\Delta Cq_{3'-5'}$ , and  $\Delta Cq_{3'-HKG}$  are proprietary and not disclosed at the request of the assay manufacturer.

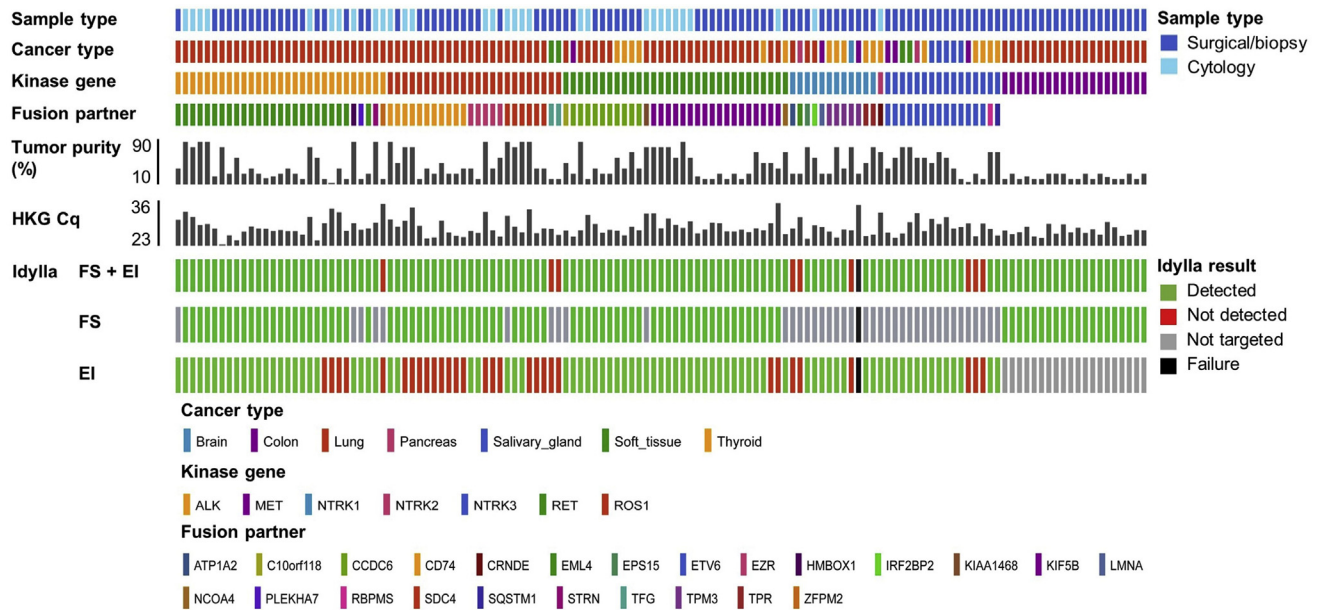


**Figure 4** Accuracy study. Plot summarizes the results of the 133 positive cases by sample type, cancer type, kinase gene, and fusion partner. Results are correlated with the tumor purity and corresponding  $C_{q_{\text{HGK}}}$  as a surrogate for RNA quality/quantity. Idylla results are stratified on the basis of consensus results of the fusion-specific primers and expression imbalance (FS + EI) and independently by modality (FS or EI). All *ALK* fusions missed by expression imbalance were associated with samples of low tumor content or low template (high  $C_{q_{\text{HGK}}}$ ) but rescued by the FS primers because of higher limit of detection of specific targeting. By contrast, 71% of *ROS1* fusions were not detected by EI primarily because of high intrinsic *ROS1* expression of the wild-type gene. All targeted non–small-cell lung cancer *ROS1* fusions were detected by the FS primers; two *ROS1* fusions not detected by the combination of FS + EI were inflammatory myofibroblastic tumors (nontargeted *TFG* partner) with tumor <20%. *NTRK* fusions, only targeted by EI, had variable expression imbalance regardless of tumor proportion. All *RET* fusions and *MET* exon 14 skipping were detected.

### Assessment of Assay Detection Limits

Assessment of limit of detection (LOD) and minimal input studies were performed using commercially available RNA reference material as well as previously characterized FFPE clinical samples.

The Seraseq Fusion RNA Mix version 4 (SeraCare, Milford, MA) was initially employed to assess overall performance parameters and the detection limits for *ALK*, *RET*, and *ROS1* fusions and for *MET* exon 14 skipping. The commercially available reference material contains biosynthetic RNA of fusion constructs (18 fusions) at known levels and RNA from a well-characterized GM24385 cell line as background wild-type material. Digital PCR-quantitated transcript concentrations and a list of included fusions are available from the manufacturer. The manufacturer additionally provided the transcript concentration of house-keeping gene *GUSB* as 15,520 copies per microliter. Of note, *NTRK2* fusions are not included in this reference material. Moreover, the constructs of its *RET*, *ROS1*, *NTRK1*, and *NTRK3* fusion transcripts did not contain the 3' probe binding sites of the Idylla GeneFusion assay. For analytic sensitivity determination, the reference material was serially diluted using RNA from a wild-type cell line (Sera-seq TNA WT Mix; SeraCare) to obtain 50%, 25%, 12.5%, 6.25%, and 3% mixtures of the starting material. Similar sensitivity determination studies were additionally performed using mixtures of FFPE tissue sections (25 mm<sup>2</sup>, 5

µm thick) from fusion-positive clinical samples with wild-type tissue from a separate tumor block to achieve tumor proportions of approximately 50%, 25%, 12.5%, 6.25%, and 3%. Minimum input studies were also performed using decreasing amounts of commercial reference RNA (200, 100, 75, 50, 40, 30, 20, 10, and 5 ng) and decreasing FFPE tissue from clinical cases starting with 1 cm<sup>2</sup> (surface area of 10 × 10 mm, 5 µm thick section) down to 6.25 mm<sup>2</sup> (surface area of 2.5 × 2.5 mm, 5 µm thick section).

### Genomic Data Visualization and Statistical Analysis

Kinase gene fusions and *MET* exon 14 skipping alterations were visualized using the ProteinPaint web application<sup>41</sup> and R version 4.0.3 (R Foundation for Statistical Computing; <https://www.r-project.org>), including package *scatterplot3d*.<sup>42</sup> Statistical analysis was performed using Microsoft Excel 2016 (Redmond, WA).

### Results

A total of 143 unique patient samples were analyzed (112 surgical and 31 cytologic specimens), including 108 NSCLCs and 35 nonlung tumors to further enrich for rare fusion partners. Table 1 summarizes the clinicopathologic characteristics of the 133 positive cases harboring a broad range of fusions and *MET* exon 14 skipping alterations

(Figure 2), as well as 10 negative NSCLC samples. Transcript identifiers are listed in Supplemental Tables S1 and S2.<sup>40</sup> Among the positive cases, 58 had distant metastases at initial presentation and 55 had received matched targeted therapy at the time of chart review. Compared with the NGS platforms, which required a turnaround time of several days to weeks, the Idylla assay was performed within 3 hours, including 2 to 3 minutes of hands-on time and without pre-extraction or batching requirements.

Supplemental Table S3 summarizes the specimen characteristics and impact on the performance of Idylla GeneFusion. Of 143 samples tested, 142 showed valid, interpretable fluorescent profiles with  $C_{q_{\text{HKG}}}$  ranging from 23.4 to 35.1 (median, 27.9; distribution displayed in Figure 3A). One surgical sample failed because of low amplification and insufficient material for retesting. High  $C_{q_{\text{HKG}}}$  values were associated with low tissue input and increased age of the samples (Figure 3B). Three cytology cases were repeated with double the input because of high  $C_{q_{\text{HKG}}}$  values ( $>30$ ) on initial testing. However, doubling the input showed similar results ( $C_{q_{\text{HKG}}}$  changed from 34.5 to 35.1, from 32.1 to 32.2, and from 32.0 to 31.6). Overall, the assay was successfully performed in samples aged up to 5 years and with inputs as low as 9 mm<sup>2</sup> for surgical specimens, or with at least 9000 cells from cytologic specimens.

## Accuracy Assessment

The accuracy study is summarized in Figure 4 and Table 2. The overall concordance with IMPACT as the reference method was 94% (133/142). Concordance was highest for *RET* fusions and *MET* exon 14 skipping alterations (100%), followed by *ALK* (99%; 141/142), *ROS1* (99%; 140/142), and *NTRK1/2/3* (96%; 136/142) fusions. Detection of fusions by FS and EI, in combination, demonstrated high specificity (100% for all targets) and sensitivity [97% (28/29) for *ALK*, 100% (31/31) for *RET*, and 92% (22/24) for *ROS1*]. Detection of alterations specifically targeted by the FS primers was also 100% for all targets, and none of the samples demonstrated nonspecific transcript amplification. In contrast, assessment by EI alone was associated with reduced sensitivity of 83% (24/29), 29% (7/24), and 94% (29/31) for *ALK*, *ROS1*, and *RET* fusions, respectively. *NTRK1/2/3* fusions, assessed only by EI, had the lowest overall sensitivity of all markers at 79% (22/28) when compared with MSK-IMPACT.

To further assess gene expression variability,  $\Delta C_{q_{3\text{'-HKG}}}$  was plotted against  $\Delta C_{q_{5\text{'-HKG}}}$  (indicators of normalized expression levels of 3' and 5' transcripts, respectively) for all cases with valid 3' and 5' curves (Figure 3C). This produced distinct clustering of *ALK* and *RET* fusion—positive and wild-type samples. Conversely, *ROS1* wild-type samples generally exhibited high levels of *ROS1* expression, which limited the distinction of *ROS1*-rearranged tumors by 3' to 5' EI. Samples harboring *NTRK* fusions showed variable

degree of 3' overexpression, limiting detection of EI in a subset of samples, regardless of tumor content.

A detailed description of all discordances in this study is presented in Supplemental Table S4. Briefly, one *ALK* fusion was not detected by Idylla (nontargeted partner *ZFPM2*) and corresponded to a case with marginal amplification ( $C_{q_{\text{HKG}}}$ , 34.9) and relatively low tumor fraction (21%). Corresponding IHC was equivocal, and FISH was positive; MSK-Fusion failed because of low coverage, reflecting a low-quality template. Four additional *ALK* fusions were not detected by EI, primarily associated with low tumor content ( $<20\%$ ), but were all detected by FS primers targeting *EML4::ALK*. Of note, one fusion initially characterized as a *RAB5C:ALK* (nontargeted partner) based on DNA testing by MSK-IMPACT was detected by both the FS and EI primers and further confirmed by MSK-Fusion as an *EML4:ALK* fusion. Two *ROS1* fusions (nontargeted *TFG* partner, inflammatory myofibroblastic tumors) were not detected by EI, both with tumor content of  $<20\%$ . Fifteen additional *ROS1* fusion cases (tumor range, 20% to 90%) were not detected by EI but were all rescued by FS targeting and detection. Only one of three nontargeted *ROS1* fusions was detected by EI (*SDC4::ROS1* exon 5:34). Finally, six *NTRK* fusions were not detected by EI despite adequate amplification, including two cases with low tumor content ( $\leq 20\%$ ). Among these, one harbored *ATP1A2::NTRK1* by MSK-IMPACT. However, the fusion was not detected at the RNA level by MSK-Fusion despite high tumor content and passing quality metrics (Supplemental Figure S2). This sample also harbored a sensitizing *EGFR* mutation (exon 19, 15-bp deletion) and the patient responded to osimertinib. On the basis of this, the fusion was interpreted to represent a non-productive rearrangement, slightly raising the sensitivity of the assay for *NTRK* fusions to 81% (22/27).

## Reproducibility

Seven clinical FFPE samples were tested in triplicate to evaluate interassay reproducibility (Supplemental Table S5). Both FS- and EI-based detection demonstrated satisfactory precision in terms of indicator values ( $C_{q_{\text{FS}}}$  and  $\Delta C_{q_{3\text{'-5'}}$ ) and the overall assay conclusions. No false positivity was observed during the reproducibility study.

## Analytic Sensitivity

The initial assessment of LOD performed on extracted RNA from reference material (SeraSeq Fusion RNA Mix version 4) is summarized in Supplemental Tables S6 and S7. Using 200 ng of extracted RNA as a fixed input,  $C_{q_{\text{HKG}}}$  values were maintained at  $<30$ , closely approximating the median  $C_{q_{\text{HKG}}}$  values when using unextracted material from one tumor tissue section (5  $\mu\text{m}$  thick) with surface area of 25 mm<sup>2</sup>. Fusion detection by FS primers was consistently possible for all markers down to the 6% dilution and further detectable at 3% for *ROS1* and *RET*. Detection by EI (for *ALK* only) was

**Table 2** Performance Summary of the Idylla GeneFusion Assay (*N* = 142 Cases after Excluding a Case with Assay Failure)

Kinase gene	MSK-IMPACT		Idylla GeneFusion				Cq <sub>FS</sub> <sup>‡</sup>	ΔCq <sub>3'-5'</sub> <sup>‡</sup>
	Pos*	Neg	Pos	Neg	Cq <sub>HKG</sub> <sup>†</sup>			
<i>ALK</i>	29/24	113	28	114	<b>28.1 (23.4 to 34.9)</b> /27.9 (25.3 to 35.1)	28.4 (24.2 to 32.6)	<b>-5.3 (-9.6 to -3.7)</b> /-1.0 (-4.0 to 6.9)	
<i>ROS1</i>	24/21	118	22	120	<b>27.8 (25.4 to 33.9)</b> /27.9 (23.4 to 35.1)	26.9 (23.3 to 32.7)	<b>-0.7 (-6.6 to 0.5)</b> /0.3 (-2.0 to 1.1)	
<i>RET</i>	31/28	111	31	111	<b>27.9 (25.9 to 35.1)</b> /28.0 (23.4 to 34.9)	27.3 (24.2 to 31.0)	<b>-2.4 (-5.3 to 1.0)</b> /2.0 (0.0 to 3.8)	
<i>NTRK1</i>	11/NA	131	8	134	<b>27.6 (25.3 to 31.2)</b> /28.0 (23.4 to 35.1)	NA	<b>-3.3 (-4.6 to 0.4)</b> /0.3 (-2.5 to 1.3)	
<i>NTRK2</i>	1/NA	141	1	141	<b>32.5</b> /27.9 (23.4 to 35.1)	NA	<b>0.13</b> /3.7 (1.4 to 5.9)	
<i>NTRK3</i>	16/NA	126	13	129	<b>28.3 (25.6 to 32.4)</b> /27.9 (23.4 to 35.1)	NA	<b>-1.4 (-3.6 to 0.4)</b> /0.6 (-0.2 to 1.4)	
<i>MET</i>	20/20	122	20	122	<b>27.3 (25.6 to 30.0)</b> /28.1 (23.4 to 35.1)	26.4 (22.0 to 29.2)	NA	
Δex14								

(table continues)

\*Total number/number harboring fusions targeted by the Idylla FS probes.

†Median (range) for fusion-positive (boldfaced)/fusion-negative cases.

‡Median (range) values for targeted cases.

Cq, quantification cycle; Δex14, Exon 14 skipping; EI, expression imbalance; FS, fusion specific; HKG, housekeeping gene; NA, not applicable; Neg, negative; NPV, negative predictive value; Pos, positive; PPV, positive predictive value.

possible for dilutions of ≥25%. With lower template input of 100 ng (Cq<sub>HKG</sub> values of approximately 31), the LOD of *ALK* was markedly affected with FS detection only above the 25% dilution and EI above 50%. For *ROS1*, *RET*, and *MET*, FS detection was unaffected. EI was not evaluable because of the absence of 3' probe binding sites on the constructs included in the commercial control material.

To further assess the performance of FFPE material, four previously characterized clinical samples harboring fusions involving *ALK*, *RET*, and *ROS* and *MET* exon 14 skipping were tested. Selected areas of each tumor, 25 mm<sup>2</sup> surface area (5 × 5 mm; 5 μm thick section), were tested, sequentially mixing with FFPE tissue from another block (wild type for the variant) to reach approximate tumor proportions down to 3%, as summarized in Supplemental Table S8. Results demonstrate that using a fixed input of at least 25 mm<sup>2</sup>, fusions can be effectively detected down to approximately 10% tumor proportion and even below if targeted by FS primers. Detection by EI is variably affected when tumor is <20%.

### Minimal Input Study

Using extracted RNA from the commercial control at decreasing total inputs of 200, 100, 75, 50, 40, 30, 20, and 10 ng (Supplemental Table S9) demonstrates the Cq<sub>HKG</sub> sequentially increases from <30 at 200 ng to approximately 34 at 10 ng, reflecting the increased number of cycles required for detectable amplification. Testing with 5 ng yielded a failure across all chambers. In this undiluted sample with fusion transcripts present at approximately 15% to 20% (normalized to housekeeping gene *GUSB* expression), all fusions and *MET* exon 14 alterations were detectable with FS primers down to the 10-ng input, corresponding to at least 673, 1112, 1967, and 578 variant

copies of *ALK*, *RET*, *ROS1* fusions, and *MET* exon 14 skipping, respectively, based on corresponding digital PCR assessment. EI for *ALK* was also detected at all levels but was not evaluable for other fusions.

Similar studies were performed on FFPE tissue sections from two clinical cases with tumor content at 50% and 20%, harboring *RET* and *ALK* fusions, respectively. Sequential decreases in the input (surface of 1 cm<sup>2</sup>, 50 mm<sup>2</sup>, 25 mm<sup>2</sup>, or 6.5 mm<sup>2</sup>) showed sequential increases of the Cq<sub>HKG</sub> from 29.9 to 34.8. In both cases, detection by FS primers was maintained at all inputs except the lowest (6.25 mm<sup>2</sup>), but detection of EI was variably compromised as the Cq<sub>HKG</sub> increased above 31. Detailed results are included in Supplemental Table S10.

### Discussion

This study assessed the clinical utility and performance of the Idylla GeneFusion assay for rapid detection of targetable fusions involving *ALK*, *ROS1*, *RET*, and *NTRK1/2/3* and *MET* exon 14 skipping mutations. This RNA-based approach delivers results in 3 hours and provides several practical benefits for both routine and clinical trial screening. These include swifter triaging of patients with advanced disease to matched targeted therapies, particularly those who are symptomatic or whose cancer is extensive, and the accelerated identification of patients for neoadjuvant or adjuvant targeted therapies in the nonmetastatic setting.

Compared with IHC, the assay delivers similar robustness for *ALK* fusion detection, while providing concurrent assessment of other relevant fusions in less time and with higher specificity. In contrast to other routine molecular methods, which require highly specialized laboratory setups

**Table 2.** (continued)

Idylla GeneFusion						
Sensitivity, % (n/total)						Overall concordance, % (n/total)
FS	EI	FS + EI	Specificity, %	PPV, %	NPV, %	
100 (25/25)	83 (24/29)	97 (28/29)	100	100	99	99 (141/142)
100 (21/21)	29 (7/24)	92 (22/24)	100	100	98	99 (140/142)
100 (28/28)	94 (29/31)	100 (31/31)	100	100	100	100 (142/142)
NA	73 (8/11)	73 (8/11)	100	100	98	98 (139/142)
NA	100 (1/1)	100 (1/1)	100	100	100	100 (142/142)
NA	81 (13/16)	81 (13/16)	100	100	98	98 (139/142)
100 (20/20)	NA	100 (20/20)	100	100	100	100 (142/142)

and a median turnaround time of several days to weeks, an Idylla microfluidic device automatically completes nucleic acid extraction, reverse transcription, qPCR, and algorithmic interpretation of multichannel fluorescent outputs in 3 hours. Single patient testing can be performed on demand without the need for batching, facilitating its use at institutions with low patient volume and flexible operation during weekends and after hours, ultimately enabling prompt clinical decision making. Technically, the assay provides highly specific and sensitive assessment for the intended alterations with similar success rates as those reported for commonly used amplicon-based NGS and NanoString assays, which range from 74% to 99%, depending on the assay.<sup>22–26,30,31</sup> By design, and in contrast to the NGS assays, the specific partner cannot be ascertained.

A notable advantage of the assay is the minimal tissue requirements, allowing the concurrent performance of both DNA and RNA assays in limited samples. Unlike most other methods that require pre-analysis RNA extraction, the Idylla cartridges accept direct input of FFPE tissue, minimizing nucleic acid loss associated with standard extraction processing. A single tissue section with surface area of  $\geq 9$  mm<sup>2</sup> (5  $\mu$ m thick) and  $\geq 20\%$  tumor can generally pass the required quality metrics for successful analysis. By contrast, if RNA was pre-extracted through routine methods, input requirements would be far greater (several slides,  $\geq 200$  ng) to reach similar quality parameters. In our hands, older FFPE samples (up to 5 years old), which would generally lead to failures by other methods due to partial RNA degradation and limited effective RNA template, still provided suitable results, although higher inputs were used ( $\geq 48$  mm<sup>2</sup> for tissue and  $>20,000$  cells for cytologic samples) compared with recent samples. In clinical practice, although most samples routinely tested are recent samples

for immediate clinical decision making, the success of older samples attests to the possibility of testing highly degraded material with acceptable success rate. Testing of old samples may also be needed in selected cases for staging purposes and discrimination of recurrences versus new primaries. The performance of cytology preparations may vary widely depending on the density of the cell pellets, and several slides are required. In our experience, for new FFPE material, approximately 9000 cells in a maximum of five unstained sections were technically sufficient. For scant samples, additional slides did not improve quality metrics or detection.

Similar to previously reported RNA hybridization-based detection (NanoString<sup>22</sup>), RT-qPCR,<sup>21</sup> matrix-assisted laser desorption/ionization time-of-flight,<sup>24</sup> and RNA-based NGS methods,<sup>30,31,43</sup> the Idylla GeneFusion assay queries kinase gene rearrangements by dual analytic strategies: FS qPCR and 3' to 5' EI. The Idylla FS probes have been designed to cover 37 predominant kinase breakpoints in lung adenocarcinomas (93%, 97%, and 85% of *ALK*, *ROS1*, and *RET* fusions) (Supplemental Table S1<sup>40</sup>). Detection by FS primers is particularly tolerant of low tumor purity and low tissue quantity. In our cohort, FS probes demonstrated 100% sensitivity and specificity toward targeted rearrangements and all *MET* exon 14 skipping alterations, even in samples with tumor as low as 14% and with high Cq<sub>HKG</sub> of 35. Detection below this level is possible, as demonstrated in our LOD study with detection down to 3% tumor.

The use of expression imbalance is a valuable complement for detection of less common fusions. We observe, however, that expression can be highly variable depending on the gene and the fusion product and is also highly affected by low tumor content compared with

fusion-specific targeting. In this cohort, EI was undetectable in all samples with <20% tumor and was limited by low template amplification ( $C_{q_{\text{HKG}}}$  above 30) and was equally supported by our LOD and minimal input studies. Therefore, negative results in samples with these characteristics should be interpreted with caution and should prompt confirmation by an alternate method. At a broader level, and unlike *ALK* and *RET*, which consistently displayed low expression in the nonrearranged genes, wild-type *ROS1* demonstrated high endogenous expression, which precluded the establishment of reliable cutoff points. Similar findings have been reported by Lira et al<sup>22</sup> using the NanoString assay on a cohort of 295 NSCLC specimens, demonstrating highly sensitive and specific detection of *ALK* and *RET* fusions by EI (sensitivity, 97% and 100%; specificity, 99% and 100%, respectively), whereas *ROS1* fusions experienced obscured 3' overexpression in the context of elevated levels of endogenous *ROS1* transcript.<sup>22</sup> Conversely, *NTRK* expression was low in wild-type samples but variable in fusion-positive samples in our study, which, together with the absence of FS targeting, contributed to a relatively low sensitivity of approximately 80%. Our assessment of *NTRK* fusions in lung cancer was limited by a low number of *NTRK* fusion-positive samples (*NTRK2* in particular; ie, not a common event) and the lack of a 3' binding site in the commercially available control that was used for our LOD studies. Literature search also suggests that the utility of EI-based detection of *NTRK* fusions remains largely uncharacterized. We identified 12 cases that underwent NanoString nCounter testing with poor correlation with pan-TRK IHC,<sup>44–46</sup> whereas qPCR-based methods have not been explored. Further studies are therefore warranted.

Altogether, and despite the described limitations in the detection of EI, the Idylla fusion assay provides a suitable solution for rapid screening of relevant fusions and *MET* exon 14 skipping alterations in lung cancers and other tumors, particularly considering the simplicity of implementation. Because of the low tissue requirements, the assay may be used in combination with other multiplex or targeted mutation assays for rapid screening, while still allowing further NGS testing in negative cases. In previous reports, we have established the high success rate of rapid screening for common mutations followed by NGS in small samples and confirm with this study that the addition of rapid RNA testing remains a feasible approach.<sup>47,48</sup> We further highlight that the use of an RNA-based assay for lung cancer patients represents an important adjunct to any routine DNA-based testing. Interrogation of DNA alone may experience several underlying genomic complexities that can lead to false-negative gene fusion results, such as limitations in tiling introns due to their large size or the presence of highly repetitive regions. At the same time, novel gene fusions detected at the DNA level may not be productive

or transcriptionally active. Although full confirmation of the significance of novel fusions would remain unclear without functional analysis, rapid RNA-based testing may be highly valuable to confirm the presence of a fusion transcript and aid in guiding immediate therapeutic decisions. Similarly, DNA-based screening for *MET* exon 14 alterations may be challenging in routine practice because of the high heterogeneity and variable location of mutations within the intron and because not all lead to exon 14 skipping. RNA testing markedly simplifies this assessment as it specifically documents the absence of a transcribed exon 14 rather than the presence of the alteration.

## Supplemental Data

Supplemental material for this article can be found at <http://doi.org/10.1016/j.jmoldx.2022.03.006>.

## References

1. Lee SE, Lee B, Hong M, Song JY, Jung K, Lira ME, Mao M, Han J, Kim J, Choi YL: Comprehensive analysis of *RET* and *ROS1* rearrangement in lung adenocarcinoma. *Mod Pathol* 2015, 28:468–479
2. Pan Y, Zhang Y, Li Y, Hu H, Wang L, Li H, Wang R, Ye T, Luo X, Zhang Y, Li B, Cai D, Shen L, Sun Y, Chen H: *ALK*, *ROS1* and *RET* fusions in 1139 lung adenocarcinomas: a comprehensive study of common and fusion pattern-specific clinicopathologic, histologic and cytologic features. *Lung Cancer* 2014, 84:121–126
3. Tuna M, Amos CI, Mills GB: Molecular mechanisms and pathobiology of oncogenic fusion transcripts in epithelial tumors. *Oncotarget* 2019, 10:2095–2111
4. Jordan EJ, Kim HR, Arcila ME, Barron D, Chakravarty D, Gao J, et al: Prospective comprehensive molecular characterization of lung adenocarcinomas for efficient patient matching to approved and emerging therapies. *Cancer Discov* 2017, 7:596–609
5. Solomon JP, Linkov I, Rosado A, Mullaney K, Rosen EY, Frosina D, Jungbluth AA, Zehir A, Benayed R, Drilon A, Hyman DM, Ladanyi M, Sireci AN, Hechtman JF: *NTRK* fusion detection across multiple assays and 33,997 cases: diagnostic implications and pitfalls. *Mod Pathol* 2020, 33:38–46
6. Awad MM, Oxnard GR, Jackman DM, Savukoski DO, Hall D, Shivdasani P, Heng JC, Dahlberg SE, Jänne PA, Verma S, Christensen J, Hammerman PS, Sholl LM: *MET* exon 14 mutations in non-small-cell lung cancer are associated with advanced age and stage-dependent *MET* genomic amplification and c-met overexpression. *J Clin Oncol* 2016, 34:721–730
7. Kim H, Jang SJ, Chung DH, Yoo SB, Sun P, Jin Y, Nam KH, Paik JH, Chung JH: A comprehensive comparative analysis of the histomorphological features of *ALK*-rearranged lung adenocarcinoma based on driver oncogene mutations: frequent expression of epithelial-mesenchymal transition markers than other genotype. *PLoS One* 2013, 8:e76999
8. Kitazawa S, Kobayashi N, Ueda S, Enomoto Y, Inoue Y, Shiozawa T, Sekine I, Kawai H, Noguchi M, Sato Y: Successful use of extracorporeal membrane oxygenation for airway-obstructing lung adenocarcinoma. *Thorac Cancer* 2020, 11:3024–3028
9. Ding L, Chen C, Zeng YY, Zhu JJ, Huang JA, Zhu YH: Rapid response in a critical lung adenocarcinoma presenting as large airway stenoses after receiving stent implantation and sequential rebiopsy guided *ALK* inhibitor therapy: a case report. *J Thorac Dis* 2017, 9: E230–E235

10. Nakashima K, Demura Y, Oi M, Tabata M, Tada T, Shiozaki K, Akai M, Ishizuka T: Utility of endoscopic ultrasound with bronchoscope-guided fine-needle aspiration for detecting driver oncogenes in non-small-cell lung cancer during emergency situations: case series. *Intern Med* 2021, 60:1061–1065
11. Hibino M, Otsuka Y, Maeda K, Horiuchi S, Fukuda M, Kondo T: Diffusion-weighted magnetic resonance imaging-directed biopsy of a metastatic bone tumor: lung adenocarcinoma with ALK rearrangement. *Respir Med Case Rep* 2018, 24:170–172
12. Gozzi E, Angelini F, Rossi L, Leoni V, Trenta P, Cimino G, Tomao S: Alectinib in the treatment of ocular metastases of ALK rearranged non small cell lung cancer: description of 2 case reports. *Medicine (Baltimore)* 2020, 99:e21004
13. Chou A, Fraser S, Toon CW, Clarkson A, Sioson L, Farzin M, Cussigh C, Aniss A, O'Neill C, Watson N, Clifton-Bligh RJ, Learoyd DL, Robinson BG, Selinger CI, Delbridge LW, Sidhu SB, O'Toole SA, Sywak M, Gill AJ: A detailed clinicopathologic study of ALK-translocated papillary thyroid carcinoma. *Am J Surg Pathol* 2015, 39:652–659
14. Park G, Kim TH, Lee HO, Lim JA, Won JK, Min HS, Lee KE, Park DJ, Park YJ, Park WY: Standard immunohistochemistry efficiently screens for anaplastic lymphoma kinase rearrangements in differentiated thyroid cancer. *Endocr Relat Cancer* 2015, 22:55–63
15. Solomon JP, Hechtman JF: Detection of NTRK fusions: merits and limitations of current diagnostic platforms. *Cancer Res* 2019, 79:3163–3168
16. Yang SR, Aypar U, Rosen EY, Mata DA, Benayed R, Mullaney K, Jayakumar G, Zhang Y, Frosina D, Drilon A, Ladanyi M, Jungbluth AA, Rekhtman N, Hechtman JF: A performance comparison of commonly used assays to detect RET fusions. *Clin Cancer Res* 2021, 27:1316–1328
17. Nozaki Y, Yamamoto H, Iwasaki T, Sato M, Jiomaru R, Hongo T, Yasumatsu R, Oda Y: Clinicopathological features and immunohistochemical utility of NTRK-, ALK-, and ROS1-rearranged papillary thyroid carcinomas and anaplastic thyroid carcinomas. *Hum Pathol* 2020, 106:82–92
18. Shan L, Jiang P, Xu F, Zhang W, Guo L, Wu J, Zeng Y, Jiao Y, Ying J: BIRC6-ALK, a novel fusion gene in ALK break-apart FISH-negative lung adenocarcinoma, responds to crizotinib. *J Thorac Oncol* 2015, 10:e37–e39
19. Mondaca S, Lebow ES, Namakydoust A, Razavi P, Reis-Filho JS, Shen R, Offin M, Tu HY, Murciano-Goroff Y, Xu C, Makhnin A, Martinez A, Pavlakis N, Clarke S, Itchins M, Lee A, Rimner A, Gomez D, Rocco G, Chaft JE, Riely GJ, Rudin CM, Jones DR, Li M, Shaffer T, Hosseini SA, Bertucci C, Lim LP, Drilon A, Berger MF, Benayed R, Arcila ME, Isbell JM, Li BT: Clinical utility of next-generation sequencing-based ctDNA testing for common and novel ALK fusions. *Lung Cancer* 2021, 159:66–73
20. Wang Y, Tian PW, Wang WY, Wang K, Zhang Z, Chen BJ, He YQ, Li L, Liu H, Chuai S, Li WM: Noninvasive genotyping and monitoring of anaplastic lymphoma kinase (ALK) rearranged non-small cell lung cancer by capture-based next-generation sequencing. *Oncotarget* 2016, 7:65208–65217
21. Aguado C, Giménez-Capitán A, Román R, Rodríguez S, Jordana-Ariza N, Aguilar A, Cabrera-Gálvez C, Rivas-Corredor C, Lianes P, Viteri S, Moya I, Molina-Vila MA: RNA-based multiplexing assay for routine testing of fusion and splicing variants in cytological samples of NSCLC patients. *Diagnostics (Basel)* 2020, 11:15
22. Lira ME, Choi YL, Lim SM, Deng S, Huang D, Ozeck M, Han J, Jeong JY, Shim HS, Cho BC, Kim J, Ahn MJ, Mao M: A single-tube multiplexed assay for detecting ALK, ROS1, and RET fusions in lung cancer. *J Mol Diagn* 2014, 16:229–243
23. Lira ME, Kim TM, Huang D, Deng S, Koh Y, Jang B, Go H, Lee SH, Chung DH, Kim WH, Schoenmakers EF, Choi YL, Park K, Ahn JS, Sun JM, Ahn MJ, Kim DW, Mao M: Multiplexed gene expression and fusion transcript analysis to detect ALK fusions in lung cancer. *J Mol Diagn* 2013, 15:51–61
24. Rogers TM, Arnau GM, Ryland GL, Huang S, Lira ME, Emmanuel Y, Perez OD, Irwin D, Fellowes AP, Wong SQ, Fox SB: Multiplexed transcriptome analysis to detect ALK, ROS1 and RET rearrangements in lung cancer. *Sci Rep* 2017, 7:42259
25. Evangelista AF, Zanon MF, Carloni AC, de Paula FE, Morini MA, Ferreira-Neto M, Soares IC, Miziara JE, de Marchi P, Scapulatempo-Neto C, Reis RM: Detection of ALK fusion transcripts in FFPE lung cancer samples by NanoString technology. *BMC Pulm Med* 2017, 17:86
26. Geiss GK, Bumgarner RE, Birditt B, Dahl T, Dowidar N, Dunaway DL, Fell HP, Ferree S, George RD, Grogan T, James JJ, Maysuria M, Mitton JD, Oliveri P, Osborn JL, Peng T, Ratcliffe AL, Webster PJ, Davidson EH, Hood L, Dimitrov K: Direct multiplexed measurement of gene expression with color-coded probe pairs. *Nat Biotechnol* 2008, 26:317–325
27. Tong Y, Zhao Z, Liu B, Bao A, Zheng H, Gu J, McGrath M, Xia Y, Tan B, Song C, Li Y: 5'/3' Imbalance strategy to detect ALK fusion genes in circulating tumor RNA from patients with non-small cell lung cancer. *J Exp Clin Cancer Res* 2018, 37:68
28. Dama E, Tillhon M, Bertalot G, de Santis F, Troglio F, Pessina S, Passaro A, Pece S, de Marinis F, Dell'Orto P, Viale G, Spaggiari L, Di Fiore PP, Bianchi F, Barberis M, Vecchi M: Sensitive and affordable diagnostic assay for the quantitative detection of anaplastic lymphoma kinase (ALK) alterations in patients with non-small cell lung cancer. *Oncotarget* 2016, 7:37160–37176
29. Liu Y, Wu S, Shi X, Lu L, Zhu L, Guo Y, Zhang L, Zeng X: Clinical evaluation of the effectiveness of fusion-induced asymmetric transcription assay-based reverse transcription droplet digital PCR for ALK detection in formalin-fixed paraffin-embedded samples from lung cancer. *Thorac Cancer* 2020, 11:2252–2261
30. Williams HL, Walsh K, Diamond A, Oniscu A, Deans ZC: Validation of the OncoPrint™ focus panel for next-generation sequencing of clinical tumour samples. *Virchows Arch* 2018, 473:489–503
31. Sakai K, Ohira T, Matsubayashi J, Yoneshige A, Ito A, Mitsudomi T, Nagao T, Iwamatsu E, Katayama J, Ikeda N, Nishio K: Performance of OncoPrint Fusion Transcript kit for formalin-fixed, paraffin-embedded lung cancer specimens. *Cancer Sci* 2019, 110:2044–2049
32. Cheng DT, Mitchell TN, Zehir A, Shah RH, Benayed R, Syed A, Chandramohan R, Liu ZY, Won HH, Scott SN, Brannon AR, O'Reilly C, Sadowska J, Casanova J, Yannes A, Hechtman JF, Yao J, Song W, Ross DS, Oultache A, Dogan S, Borsu L, Hameed M, Nafa K, Arcila ME, Ladanyi M, Berger MF: Memorial Sloan Kettering-Integrated Mutation Profiling of Actionable Cancer Targets (MSK-IMPACT): a hybridization capture-based next-generation sequencing clinical assay for solid tumor molecular oncology. *J Mol Diagn* 2015, 17:251–264
33. Benayed R, Offin M, Mullaney K, Sukhadia P, Rios K, Desmeules P, Ptashkin R, Won H, Chang J, Halpenny D, Schram AM, Rudin CM, Hyman DM, Arcila ME, Berger MF, Zehir A, Kris MG, Drilon A, Ladanyi M: High yield of RNA sequencing for targetable kinase fusions in lung adenocarcinomas with no mitogenic driver alteration detected by DNA sequencing and low tumor mutation burden. *Clin Cancer Res* 2019, 25:4712–4722
34. Robinson JT, Thorvaldsdóttir H, Winckler W, Guttman M, Lander ES, Getz G, Mesirov JP: Integrative genomics viewer. *Nat Biotechnol* 2011, 29:24–26
35. Buels R, Yao E, Diesh CM, Hayes RD, Munoz-Torres M, Helt G, Goodstein DM, Elsik CG, Lewis SE, Stein L, Holmes IH: JBrowse: a dynamic web platform for genome visualization and analysis. *Genome Biol* 2016, 17:66
36. Shen R, Seshan VE: FACETS: allele-specific copy number and clonal heterogeneity analysis tool for high-throughput DNA sequencing. *Nucleic Acids Res* 2016, 44:e131
37. Hanna MG, Reuter VE, Hameed MR, Tan LK, Chiang S, Sigel C, Hollmann T, Giri D, Samboy J, Moradel C, Rosado A, Otilano JR 3rd, England C, Corsale L, Stamelos E, Yagi Y, Schöffler PJ, Fuchs T, Klimstra DS, Sirintrapun SJ: Whole slide

- imaging equivalency and efficiency study: experience at a large academic center. *Mod Pathol* 2019, 32:916–928
38. Bankhead P, Loughrey MB, Fernández JA, Dombrowski Y, McArt DG, Dunne PD, McQuaid S, Gray RT, Murray LJ, Coleman HG, James JA, Salto-Tellez M, Hamilton PW: QuPath: open source software for digital pathology image analysis. *Sci Rep* 2017, 7:16878
  39. Tate JG, Bamford S, Jubb HC, Sondka Z, Beare DM, Bindal N, Boutselakis H, Cole CG, Creatore C, Dawson E, Fish P, Harsha B, Hathaway C, Jupe SC, Kok CY, Noble K, Ponting L, Ramshaw CC, Rye CE, Speedy HE, Stefancsik R, Thompson SL, Wang S, Ward S, Campbell PJ, Forbes SA: COSMIC: the catalogue of somatic mutations in cancer. *Nucleic Acids Res* 2018, 47:D941–D947
  40. The NCBI Handbook [Internet]. Bethesda, MD: National Library of Medicine (US), National Center for Biotechnology Information; 2002
  41. Zhou X, Edmonson MN, Wilkinson MR, Patel A, Wu G, Liu Y, Li Y, Zhang Z, Rusch MC, Parker M, Becksfort J, Downing JR, Zhang J: Exploring genomic alteration in pediatric cancer using ProteinPaint. *Nat Genet* 2016, 48:4–6
  42. Ligges U, Maechler M: scatterplot3d—An R package for visualizing multivariate data. *Journal of Statistical Software* 2003, 8:1–20
  43. Haynes BC, Blidner RA, Cardwell RD, Zeigler R, Gokul S, Thibert JR, Chen L, Fujimoto J, Papadimitrakopoulou VA, Wistuba II, Latham GJ: An integrated next-generation sequencing system for analyzing DNA mutations, gene fusions, and RNA expression in lung cancer. *Transl Oncol* 2019, 12:836–845
  44. Yamashiro Y, Kurihara T, Hayashi T, Suehara Y, Yao T, Kato S, Saito T: NTRK fusion in Japanese colorectal adenocarcinomas. *Sci Rep* 2021, 11:5635
  45. Elfving H, Broström E, Moens LN, Almlöf J, Cerjan D, Lauter G, Nord H, Mattsson JSM, Ullenhag GJ, Strell C, Backman M, La Fleur L, Brunnström H, Botling J, Micke P: Evaluation of NTRK immunohistochemistry as a screening method for NTRK gene fusion detection in non-small cell lung cancer. *Lung Cancer* 2021, 151:53–59
  46. Kurihara T, Suehara Y, Akaike K, Hayashi T, Kohsaka S, Ueno T, Hasegawa N, Takagi T, Sasa K, Okubo T, Kim Y, Mano H, Yao T, Kaneko K, Saito T: Nanostring-based screening for tyrosine kinase fusions in inflammatory myofibroblastic tumors. *Sci Rep* 2020, 10: 18724
  47. Arcila ME, Yang SR, Momeni A, Mata DA, Salazar P, Chan R, Elezovic D, Benayed R, Zehir A, Buonocore DJ, Rekhman N, Lin O, Ladanyi M, Nafa K: Ultrarapid EGFR mutation screening followed by comprehensive next-generation sequencing: a feasible, informative approach for lung carcinoma cytology specimens with a high success rate. *JTO Clin Res Rep* 2020, 1:100077
  48. Momeni-Boroujeni A, Salazar P, Zheng T, Mensah N, Rijo I, Dogan S, Yao J, Mung C, Vanderbilt C, Benhamida J, Chang J, Travis W, Rekhman N, Ladanyi M, Nafa K, Arcila ME: Rapid EGFR mutation detection using the Idylla platform: single-institution experience of 1200 cases analyzed by an in-house developed pipeline and comparison with concurrent next-generation sequencing results. *J Mol Diagn* 2021, 23:310–322